Imaging Photoplethysmography (iPPG) in Head and Neck Reconstructive Surgery

A Novel Technique for Noninvasive Flap Perfusion Monitoring

van der Stel, S. D.; Lai, M.; Groen, H. C.; Dirven, R.; Karakullukcu, M. B.; Karssemakers, L. H.E.; van Gastel, M.; Hendriks, B. H.W.; Ruers, T. J.M.; Schreuder, W. H.

DOI
10.1002/lsm.23859

Publication date
2024

Document Version
Final published version

Published in
Lasers in Surgery and Medicine

Lasers in Surgery and Medicine

PRECLINICAL STUDY OPEN ACCESS

Imaging Photoplethysmography (iPPG) in Head and Neck Reconstructive Surgery: A Novel Technique for Noninvasive Flap Perfusion Monitoring

S. D. van der Stel[1,2] | M. Lai[3,4] | H. C. Groen[2] | R. Dirven[5] | M. B. Karakullukcu[5] | L. H. E. Karssemakers[5] | M. van Gastel[4,6] | B. H. W. Hendriks[3,7] | T. J. M. Ruers[1,2] | W. H. Schreuder[5]

[1]Faculty TNW, Group Nanobiophysics, Twente University, Enschede, North Brabant, The Netherlands | [2]Department of Surgery, The Netherlands Cancer Institute—Antoni van Leeuwenhoek, Amsterdam, The Netherlands | [3]IGT & US Systems, Philips Research, High Tech, Eindhoven, The Netherlands | [4]Department of Electrical Engineering, Eindhoven University of Technology, Eindhoven, The Netherlands | [5]Department of Head and Neck Surgery and Oncology, The Netherlands Cancer Institute—Antoni van Leeuwenhoek, Amsterdam, The Netherlands | [6]Patient Care & Monitoring, Philips Research, High Tech, Eindhoven, The Netherlands | [7]Biomedical Engineering, Delft University of Technology, Delft, The Netherlands

Correspondence: S. D. Stel (s.vd.stel@nki.nl)

Received: 9 July 2024 | **Revised:** 23 September 2024 | **Accepted:** 21 October 2024

Funding: Financial support was provided the European Union's Horizon 2020 Research and Innovation Program under Marie Skłodowska-Curie (Grant 721766).

Keywords: free flap reconstruction | head and neck cancer | head and neck reconstructive surgery | imaging photoplethysmography | iPPG | oral cancer | perfusion monitoring

ABSTRACT

Background: Evaluate imaging photoplethysmography (iPPG) as a novel noninvasive technique to assess flap perfusion in head and neck free flap reconstructive (FFR) surgeries.

Methods: Intraoperative iPPG was performed in 17 patients undergoing FFR surgery. Imaging consisted of a 30-s video from which perfusion maps were extracted, providing detailed information about blood flow and pulsatility in the flap microvasculature. During each procedure, iPPG acquisitions were acquired representing distinct perfusion conditions of the flap (fully perfused/ischemic/reperfused). When possible, postoperative measurements were performed to assess flap recovery during the critical time period (3 days) and long-term follow-up (30 days).

Results: Perfusion maps, displaying iPPG amplitude and delay times, correlated strongly ($p < 0.001$) with the perfusion status of the tissue. One case of postoperative thrombosis, leading to flap failure, was identified with iPPG. After surgical revision in this case, flap perfusion was restored and confirmed by iPPG. Postoperative follow-up imaging allowed for objective visualization of flap recovery short term (3 days) and up to 30 days after the surgical procedure.

Conclusions: This study shows that iPPG is suitable for objective and noninvasive assessment of flap perfusion in head and neck FFR surgery. In addition, postoperative monitoring shows potential for assessing flap perfusion in patients with increased risk of postoperative complications.

1 | Introduction

In head and neck oncological surgery, free flap reconstruction (FFR) has become the standard of care for large and composite tissue defects. Even though FFR are long and complex procedures, reported flap success rates are well above 90% [1, 2].

Perfusion is essential for flap recovery and survival. The small risk of partial or complete flap loss due to inadequate perfusion

remains one of the most serious and feared postoperative complications, and early detection followed by immediate surgical intervention are required for successful flap salvage [3]. In case of flap failure, approximately 51% of these cases have signs of vascular compromise within the first 4 h after surgery, 82% within the first 24 h and 96% within the first 72 h [2]. During this critical time period, most clinicians apply physical examination to test flap viability, such as assessment of flap color, temperature, capillary refill, and turgor. However, these techniques are susceptible for misinterpretations and rely mainly on surgeons' experience [4]. Other methods, such as (implantable) Doppler sonography and pinprick are also frequently used for monitoring flap perfusion [5]. However, these allow only for local and superficial perfusion assessment.

In the search toward better and objective techniques for postoperative monitoring, many advances have been made [4, 6–9]. Yet, many studies fail to show evidence for clinical use, lacking flap salvage and false-positive rates [7]. Near-infrared spectroscopy (NIRS) and hyperspectral imaging (HSI) were recently assessed in detecting flap failure in reconstructive surgery [10]. Both techniques target tissue oxygenation as a measure of tissue perfusion and proved to be promising monitoring methods. However, due to the use of different wavelengths and subsequent penetration depths, and lack of a generalized system and algorithms, the interpretation of tissue oxygenation remains challenging. Hence, defining universal values is necessary before HSI and NIRS can be used in clinical care.

Imaging photoplethysmography (iPPG) is a promising noninvasive optical imaging technique. It can detect perfusion by assessing blood volume changes in the microvasculature tissue bed beneath the tissue surface [11, 12]. Previous studies have shown that iPPG can differentiate between arterial and venous compromise of a flap [7, 13, 14]. Recently, iPPG displayed promising results in accurately detecting tissue perfusion in the surgical setting [15]. Perfusion levels were displayed in color-coded perfusion maps and provided easy and fast assessment. Despite the increasing popularity and widespread research interest of iPPG, few studies have investigated the use of iPPG for tissue perfusion assessments of free flaps in head and neck reconstructive surgery [4, 7].

The main goal aim of this study is to assess the feasibility of iPPG for assessing perfusion in free flaps at various intraoperative stages during head and neck reconstructive surgeries. Moreover, when possible, we also aim to assess the perfusion changes in the transplanted tissue during flap recovery in the postoperative phase. Based on the results of the aforementioned earlier studies [15], we hypothesize that iPPG can accurately detect perfusion changes and differentiate between different perfusion states of free flaps used for head and neck reconstruction.

2 | Methods

2.1 | Study Population

In this prospective cohort study, patients scheduled for an ablative head and neck surgical procedure followed by an FFR between June 2020 and June 2022 in the Antoni van Leeuwenhoek—Netherlands Cancer Institute (AVL-NKI) hospital were included. Patients with either flap receptor locations inaccessible for adequate iPPG acquisition or flaps that did not include a cutaneous component were excluded. The study was approved by the Institutional Review Board (IRB) of the AVL-NKI and registered with the number IRBd19-155. Written informed consent for participation was provided by all patients included in the study. Data were acquired according to the IRB guidelines of the AVL-NKI. The study was performed in compliance with the Declaration of Helsinki.

2.2 | Data Collection

An iPPG setup was used, which is described in detail in our previous work [15]. In short, an off-the-shelf 2.8-Megapixels RGB camera (Manta G283B, Allied Vision Technologies GmbH, Germany) with a 52-mm objective, and an LED ring in the visible range (Falcon Eyes Macro ring-light MRC-80FV, Benèl BV, the Netherlands) equipped with a cross-polarized light filter (Edmund Optics, Visible linear polarizer) was used. Images at 20 frames per second and 12-bit color depth were acquired with the camera. For the optimal field of view, the camera was mounted on a tripod and positioned approximately 50 cm from the target tissue (Figure 1a). All lights in the operating room, including headlights of the surgeons, were switched off during the acquisition to minimize external light interferences and the flap was cleaned from excess blood. For each acquisition, the iPPG setup came in the surgical field for approximately 1 min, including positioning of the camera and acquisition. Videos of 30 s each were acquired intraoperatively for each patient at four different stages during the procedure, displaying different perfusion conditions. Before the procedure started, a region of interest was marked and imaged at the cutaneous component of the flap in situ at the donor site before initiation of harvest (*baseline*). Second, the flap was imaged when freely dissected and mobilized and only connected to the main vascular pedicle before ligation (*mobilized*). Third, when the blood vessels of the main vascular pedicle were ligated and ischemia time had started (*ischemic*), and lastly, the flap was imaged after restoration of the perfusion by microsurgical anastomosis at the receptor site (*reperfused*). When possible, postoperative monitoring was performed to assess flap recovery during the critical time period (3 days) and during long-term follow-up (30 days) after surgery (*postoperatively*). To not influence clinical decision-making, the surgeon was blinded for the results of acquisition. As standard clinical practice, flap perfusion was assessed by the surgeons via golden standard (pinprick and clinical assessment of flap color, temperature, capillary refill, and turgor).

2.3 | Data Analysis

The primary end goal of the study was to demonstrate the ability of iPPG to differentiate between perfusion levels in different perfusion states (baseline/mobilized/ischemic/reperfused) of free tissue transfers used for head and neck reconstruction. Therefore, data was processed offline in Matlab

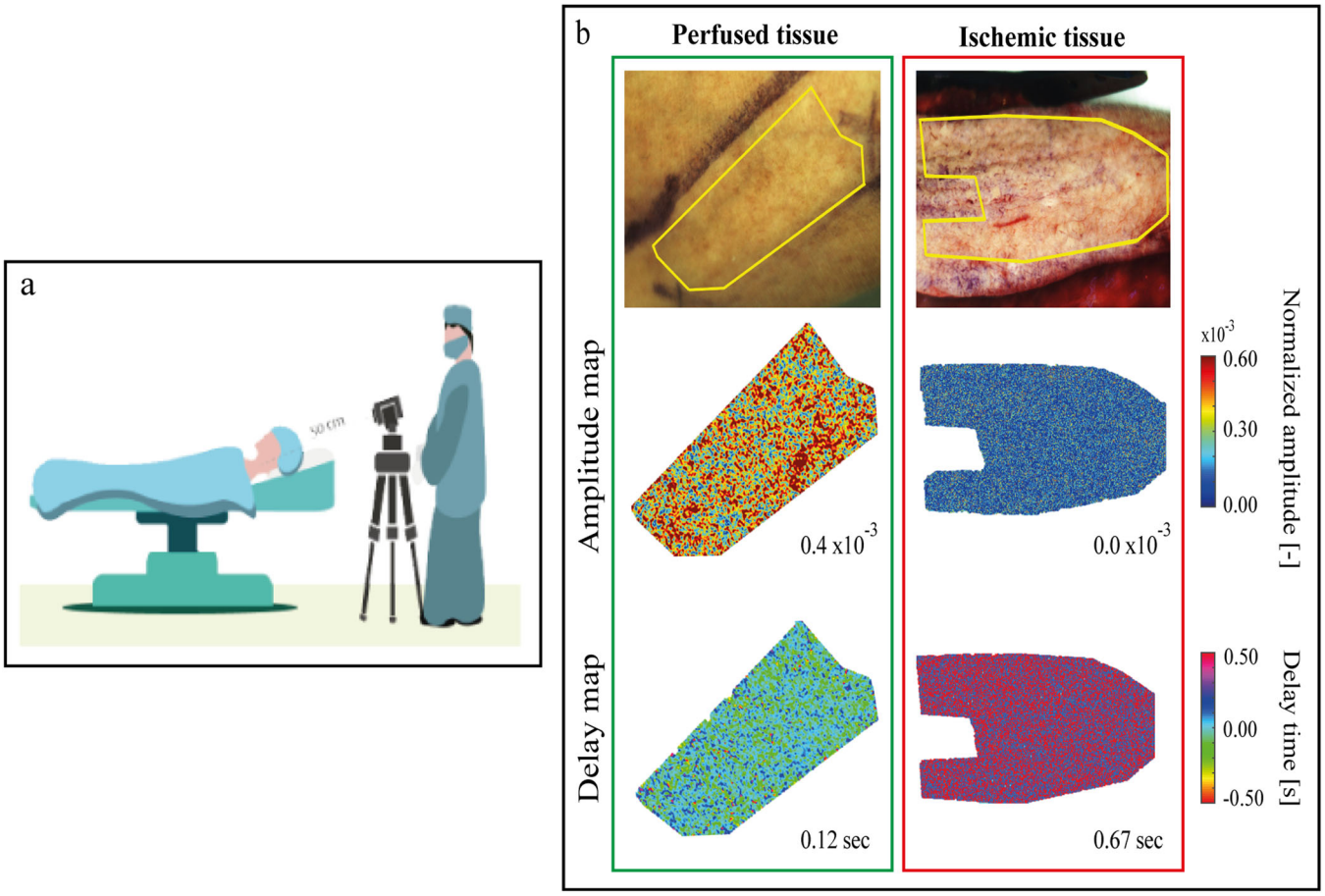

FIGURE 1 | (a) Schematic representation of the iPPG setup during surgery. For optimal acquisition, the camera is positioned approximately 50 cm from the target tissue. (b) Perfusion maps extracted after acquisition. Perfused tissues are characterized with high iPPG amplitude, characterized with yellow and red color (0.4×10^{-3}) and a uniformly distributed signal delay (0.12 s, green box), whereas ischemic tissues display low iPPG amplitude, characterized with blue color (0.0×10^{-3}), and a signal delay randomly distributed with high delay times variations (0.67 s, red box). iPPG amplitude and delay times are expressed as median values.

(R2021b, the Mathworks Inc., Massachusetts, United States) using a custom build script [15]. This software calculates perfusion maps of manually selected regions of interest (ROIs) of the imaged tissue, which can be generated within 1 min after the acquisition. Subsequently, the information from each pixel in the image is extracted using the Plane-Orthogonal-to-Skin (POS) algorithm, which exploits the fact that green light is absorbed much more by the hemoglobin in the blood rather than red and blue light. PPG signals from the red, green, and blue channels of the video were extracted, and the pulsatile component Alternating Coupling (AC) of the signal of each pixel was normalized for its baseline color component Direct Coupling (DC). This resulting amplitude of the PPG signal reflects a percentage and compensates for the parameters that affect both pulsation and baseline color level components, such as the intensity of the light or tissue color. The principle of iPPG is explained in more detail in Lai et al. [15].

iPPG-derived perfusion parameters (amplitude map and delay map) were subsequently extracted from the perfusion maps, allowing for differentiation between perfused and non-perfused regions (Figure 1b). The iPPG amplitude displays blood flow within the skin flap, and is expressed as the median due to the lack of a normal distribution in the amplitude map. The iPPG delay map identifies the iPPG signal arrival time within the tissue of interest. In well-perfused tissues, the pulsatility arrives almost simultaneously throughout the imaged tissue, and is expressed as a uniform color that indicates a delay that is close to 0 s. On the other hand, ischemic tissues display large variations within the pulsatility arrival time, leading to a random distribution in the delay map. The delay map is expressed as an interquartile range (IQR) due to its characteristic to show the spread within the delay, eliminating extreme outliers caused by inherent noise. The secondary end goal of the study was to assess the postoperative perfusion changes imaged by iPPG that occurred during short-term (Days 0–3 postoperatively) and long-term (Days 0–30 postoperatively) follow-up.

2.4 | Statistical Analysis

Statistical analysis was performed using IBM SPSS statistics v27 (SPSS Inc., Chicago, United States) and Matlab (R2021b, the Mathworks Inc., Massachusetts, United States). Quantitative data is presented as means and standard deviations, whereas qualitative data is presented as numbers and percentages. Normal distribution was assessed with the Shapiro–Wilk test. Statistical analysis was performed using a two-way ANOVA

followed by post-hoc pairwise comparison with Bonferroni correction for normally distributed data, the Wilcoxon signed-rank test was performed for non-normally distributed data. A p-value ≤ 0.05 was considered statistically significant.

3 | Results

3.1 | Population

In total 17 patients undergoing an ablative head and neck surgical procedure followed by FFR were included. Patient demographics, clinicopathologic, and reconstructive characteristics are shown in Table 1. Patients were predominantly treated for a squamous cell carcinoma of the upper aerodigestive tract (58.8%). Reconstruction was performed using either a fasciocutaneous radial forearm flap (FRFF, 58.8%), fasciocutaneous anterolateral thigh flap (ALT, 17.6%), or osteomyocutaneous fibula free flap (FFF, 23.5%). For the arterial anastomosis the facial artery was most commonly used (76.5%). The internal jugular vein was the most preferred vein for venous anastomosis (end-to-side; 100%). When a second vein was available, a second venous anastomosis was created (end-to-end; 82.4%).

3.2 | Intraoperative Flap Assessment

Flap perfusion was assessed at different stages during the surgical procedure (Figure 2). The IQR of the delay map was distributed normally ($p > 0.05$), whereas the iPPG signal amplitude was not distributed normally ($p < 0.05$). iPPG amplitude was correlated with perfusion, being high in perfused tissues and low in ischemic tissues. After revascularization of the flap, an increase in iPPG amplitude was observed compared to the preoperative situation (Figure 2a). The delay time of arrival of the iPPG signal was inversely correlated with the perfusion condition, being high in ischemic tissues and low in perfused tissues (Figure 2b).

3.3 | Postoperative Flap Assessment

Postoperative monitoring of the skin flap was conducted when the location of the flap allowed for iPPG acquisitions, and comfort for the patient could be guaranteed. In total, six patients (35%) were eligible for postoperative follow-up. To assess flap recovery, short-term (3 days) and long-term (1 month) monitoring were conducted in two patients.

3.4 | Short-Term Monitoring

During the surgical procedure, the skin flap was subjected to a period of ischemia before microscopic revascularization in the new recipient site, displayed by a drastic drop in iPPG amplitude, and increase in delay time. A perfusion rebound was observed during the postoperative monitoring period (Figure 3a). After restoring the vascularization of the flap, a large increase in amplitude levels were observed, increasing within the first 3 days postoperatively. iPPG delay time

TABLE 1 | Patient demographics.

	n	(%)
Total	17	(100)
Gender		
Male	11	(64.7)
Female	6	(35.3)
Age, years (range)	68	51–88
Smoking		
Yes	5	(29.4)
Former smoker	6	(35.3)
No	6	(35.3)
Type of surgery		
Fasciocutaneous radial forearm flap (FRFF)	10	(58.8)
Fasciocutaneous anterolateral thigh flap (ALT)	3	(17.6)
Osteomyocutaneous fibula free flap (FFF)	4	(17.6)
American Society of Anesthesiologists (ASA) score		
2	13	(76.5)
3	4	(23.5)
Ischemia time during surgery, min, mean (SD)	123	(22)
Tumor type		
Mucosal squamous cell carcinoma	10	(58.8)
Recurrent adenoid cystoid carcinoma	1	(5.9)
Salivary duct carcinoma	1	(5.9)
Adenocarcinoma base of tongue	1	(5.9)
Cutaneous squamous cell carcinoma	1	(5.9)
Osteoradionecrosis (ORN)	3	(17.6)
Tumor location		
Oral cavity	14	(82.4)
Oropharynx	1	(5.9)
Salivary duct parotid gland	1	(5.9)
Skin	1	(5.9)
Anastomosis type		
Arterial	17	
Facial artery	13	(76.5)
Superior thyroid artery	2	(11.8)
Lingual artery	1	(5.9)
Internal carotid artery	1	(5.9)
Venous 1	17	
Internal jugular vein	17	(100)
Venous 2	14	
Facial vein	13	(76.5)
External jugular vein	1	(5.9)

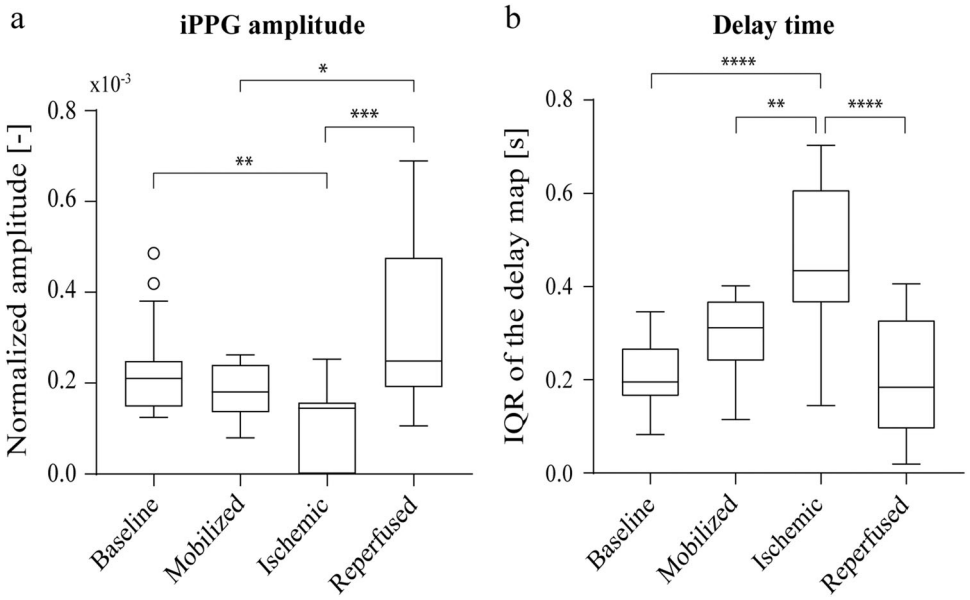

FIGURE 2 | iPPG-derived perfusion parameters. (a) iPPG amplitude is correlated with perfusion of the tissue. (b) On the other hand, delay time is inversely correlated with perfusion. (a) Values are expressed as lower/upper quartiles and min/max, (b) values are expressed as mean ± standard deviation median; *$p \leq 0.05$, **$p \leq 0.01$, ***$p \leq 0.001$, ****$p \leq 0.0001$.

displayed an inverse trend, increasing during ischemia time before returning to baseline levels after 3 days. iPPG amplitude levels experienced almost a threefold increase after 66 h compared to the preoperative levels, whereas delay times were similar to preoperative values (Figure 3b).

3.5 | Long-Term Monitoring

Additionally, long-term monitoring was performed to identify flap recovery over a longer period. Here, perfusion rebounds directly after revascularization of the flap, up to threefold the preoperative levels, and gradually decreases over time (Figure 4a). After 2 weeks, a new perfusion baseline is reached that is maintained for the remainder of the follow-up period (Figure 4b).

3.6 | Postoperative Complications

Two patients developed postoperative flap-related complications (Table 2). One patient suffered an arterial failure of the flap within 3 h after the surgical procedure (Grade IIIb complication [16]), and had to be taken back to the operating theater for exploratory surgery (Figure 5a). The surgery resulted in mechanical removal of the thrombus and thrombolytic therapy with the administration of urokinase to successfully dissolve distal microthrombi, saving the flap. After flap failure was confirmed with clinical testing, iPPG acquisitions were made. The amplitude map showed very low signal amplitude in the flap compared with the surrounding tissues (Figure 5b). After surgery, increased iPPG amplitude was observed, indicating sufficient flap perfusion (Figure 5c,d). A second patient suffered flap dehiscence after 9 days. Unfortunately, this patient was not included for the postoperative follow-up. Additionally, two patients developed general complications that did not lead to flap-related complications.

3.7 | Discussion

In the present study, free flap perfusion during and after head and neck reconstruction was for the first time assessed using noninvasive iPPG acquisitions. These iPPG acquisitions demonstrated the ability to identify variations in flap perfusion during the different perfusion conditions at specific stages during the surgical procedure. The acquisitions allowed to display perfusion in perfusion maps and enabled an easy assessment of tissue of interest. iPPG-derived parameters (iPPG amplitude and delay time) provided numerical identification of perfusion values and displayed correlation with the perfusion status of the tissue. Additionally, postoperative follow-up imaging allowed for objective visualization of flap recovery up to 30 days after the surgical procedure.

iPPG is a noninvasive imaging technique and able to detect perfusion changes within the microvasculature tissue bed [11, 12]. In the present study, iPPG was able to detect flap perfusion during surgical procedures in different perfusion conditions and during postoperative follow-up. When the flap was freely dissected and mobilized and only connected to the main vascular pedicle before ligation, the resulting vasoconstriction caused the iPPG amplitude to decrease (Figure 2a). Immediately after revascularization, a rebound in flap perfusion was observed with a threefold increase within the first 4 days postoperatively. The high demand for proinflammatory cytokines in the wound healing process [17], and the need to wash out ischemic damage [18] causes vasodilation in the flap, resulting in an increase in blood flow within the skin flap. Additionally, the new anatomical location and larger artery size may contribute toward the increased flow within the skin flap. Within days, this high

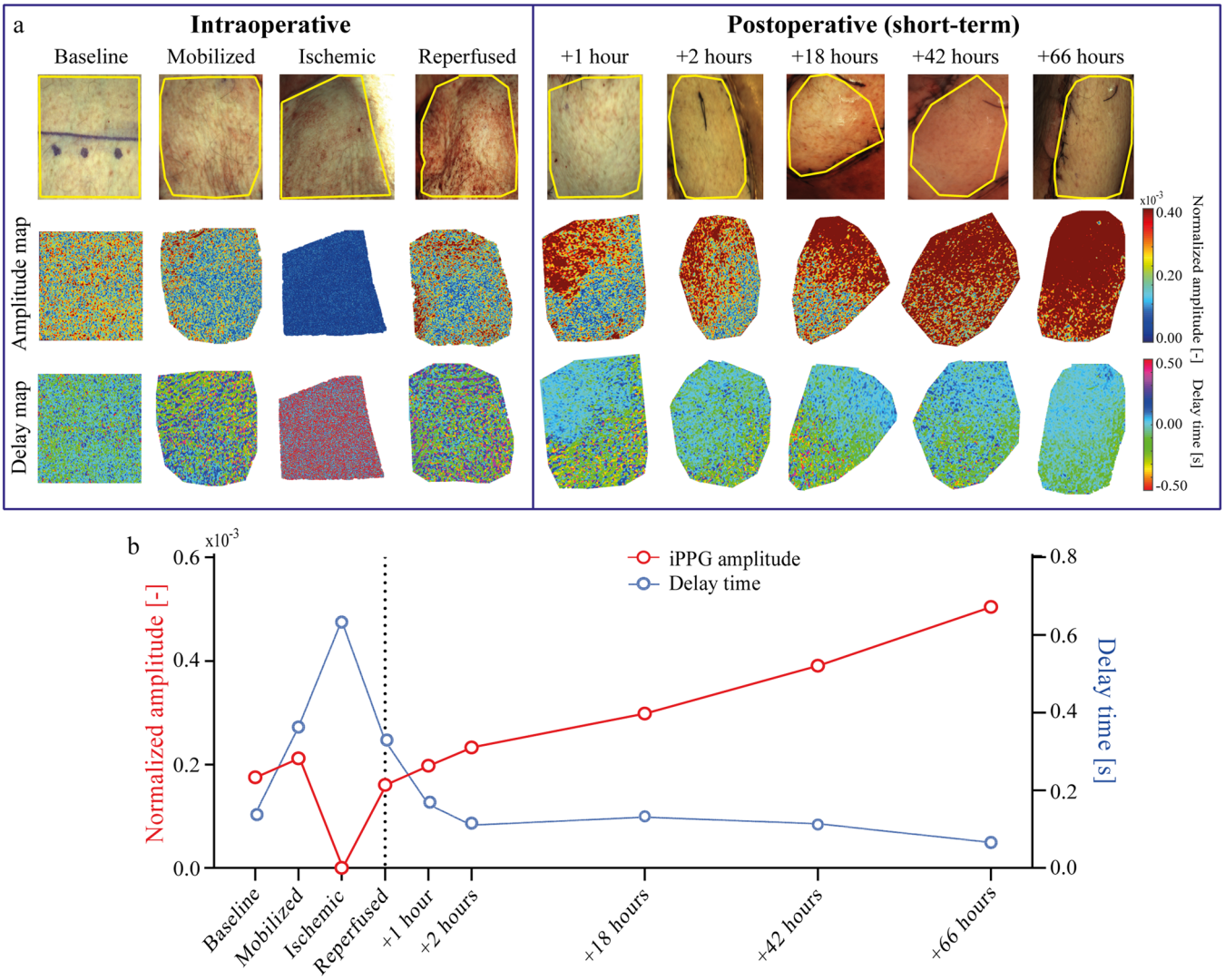

FIGURE 3 | Short-term follow-up until 3 days postoperatively in one patient receiving an FRFF. The flap is imaged at specific conditions during the surgical procedure, and postoperatively at +1, +2, +18, +42, and +66 h. (a) Intra- and postoperative images with corresponding iPPG amplitude and iPPG delay maps. iPPG amplitude drops closely to zero in the ischemic skin flap, before it rebounds after reperfusion. After 66 h, the blood supply is uniformly distributed in the flap. iPPG delay maps show an inversely correlated trend. (b) iPPG amplitude (red) and delay time (blue) plotted over time, corresponding to the maps shown in (a).

perfusion in the flap normalizes when the dependence of the anastomosis decreases as a result of neovascularization between the flap and surrounding tissues. Recent studies showed that wound healing initiates neovascularization in the wound bed [19, 20]. This leads to the flap to become independent of the pedicle blood supply 7–14 days after surgery [21]. In the present study, a normalization in perfusion was observed between 14 and 30 days postoperatively, indicating adaptation of the flap in the recipient site. This is in accordance with a recent study that found that autonomization of the flap is initiated but not yet completed 2 weeks postoperatively [22].

Two patients developed postoperative flap-related complications in this study. In one patient, flap dehiscence without (partial) flap loss occurred 9 days after surgery, requiring wound debridement and antibiotics. In another patient, after revascularization of the skin flap, clinical characteristics such as a negative pinprick and pale skin color indicated flap failure, for which surgical revision was indicated. In addition, very low iPPG amplitudes were observed (Figure 5a). This particular patient suffered a thrombus in the supplying artery of the flap within 2 h after the procedure, requiring surgical revision of the arterial anastomosis and thrombolytic treatment. Fortunately, the flap was salvaged due to immediate intervention after the detection of the thrombus, and after a secondary iPPG assessment, the flap showed no signs of compromised perfusion. iPPG-derived parameters of the failing flap displayed values which were not observed in good surgical outcomes. With these deviating values, potential indicators for inadequate flap perfusion and increased risk of flap loss can be identified, ultimately leading to a threshold for defining adequate and inadequate flap perfusion. However, based on the high success rate of FFR [23], a larger case number and control series is required to identify iPPG-derived parameter values at which flap loss is likely to occur.

Currently, Indocyanine Green (ICG) is being widely used for assessing flap perfusion intraoperatively. In the postoperative

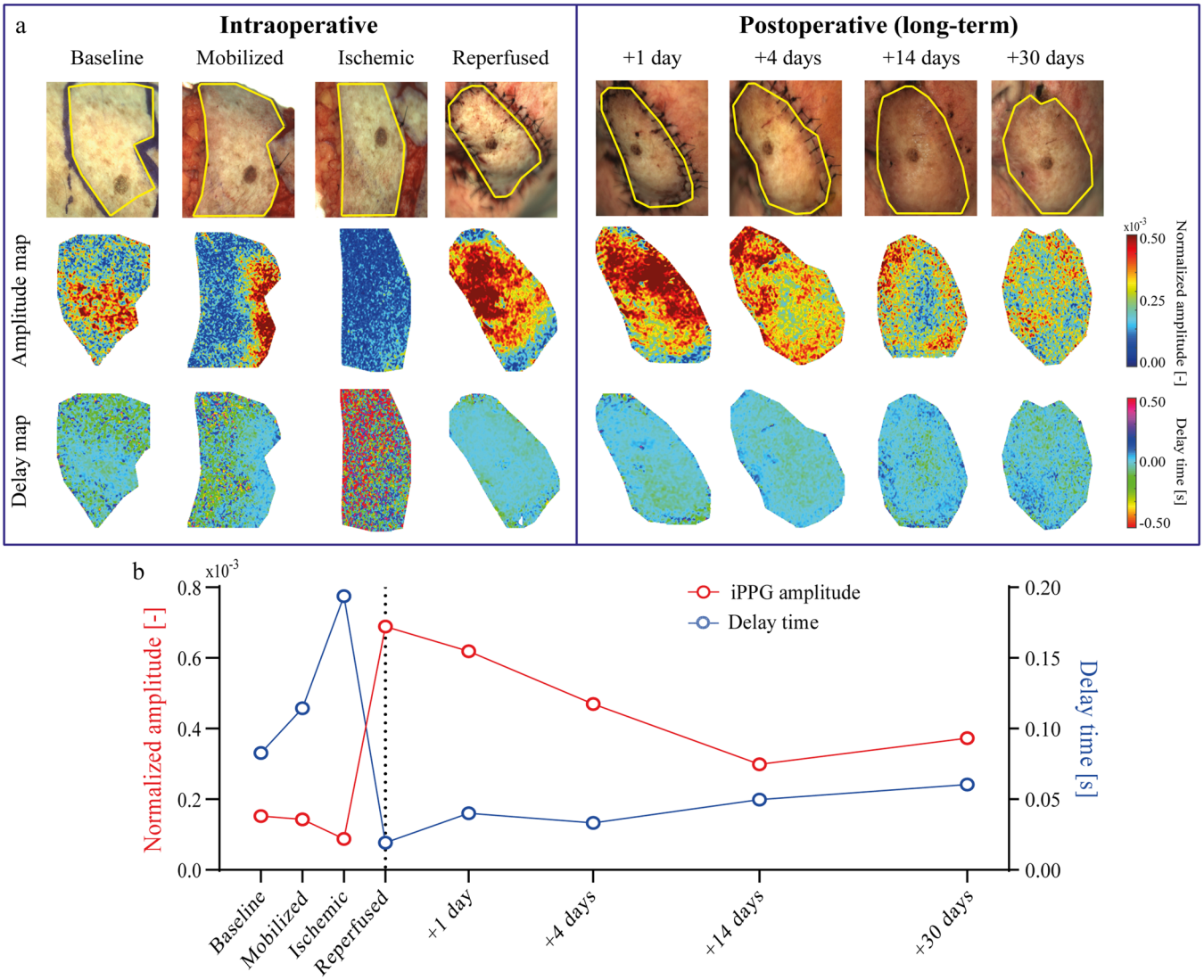

FIGURE 4 | Long-term follow-up until 30 days postoperatively in one patient receiving an FRFF. The flap is imaged at specific conditions during the surgical procedure, and postoperatively after 1, 4, 14, and 30 days. (a) Perfusion rebounds directly after reconnecting the flap blood supply in the recipient site and increases up to within the first 24 h after surgery. After 14 days, perfusion achieves a new baseline, which is higher compared to the preoperative baseline. (b) iPPG amplitude (red) and delay time (blue) plotted over time, corresponding to the maps shown in (a).

TABLE 2 | Postoperative complications.

Complication	Grade of complication	*n*	(%)
Flap-related postoperative complications			
Flap dehiscence	I	1	(5.9)
Arterial thrombus	IIIb	1	(5.9)
Other postoperative complications			
Hematoma	I	1	(5.9)
Pulmonary embolism	II	1	(5.9)
No postoperative complications		13	(76.5)

setting, ICG is not suitable due to the invasive nature of injecting the fluorescent dye necessary for each acquisition. As such, different techniques are used for postoperative monitoring, such as physical examination or (implantable) Doppler devices. However, high costs, lack of quantitative/objective values, and necessity of implanting a device are currently limiting the potential of implantable Doppler devices [24]. Furthermore, one of the main challenges with perforator-based flaps is the heterogeneous distribution of perfusion in the flap. As such, "hot zones," located in close proximity to the

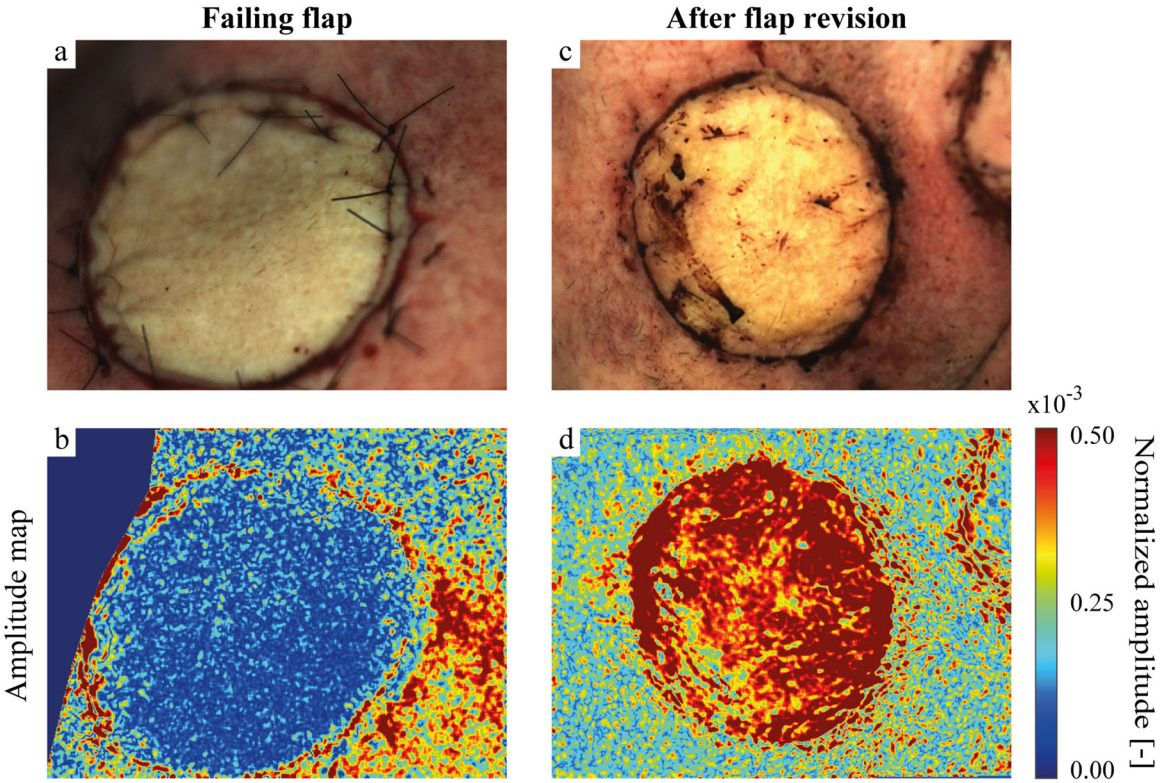

FIGURE 5 | Flap failure postoperatively. (a) In this specific case, within 3 h after surgery, flap failure was suspected due to paleness and absence of pulsations. (b) When imaged with the iPPG camera, the flap displayed extremely low iPPG amplitudes compared to surrounding tissue. During surgical revision, a thrombus was detected in the flap arterial pedicle, and subsequently treated with urokinase. (c, d) After revision surgery and restoring blood flow, iPPG amplitudes increased in the flap and no signs of compromised perfusion were detected during postoperative recovery.

perforator, and "cold zones" located distally from the perforator are described. From this standpoint, point-based, local acquisition of the perfusion can lead to a biased interpretation of the perfusion status of the complete flap, potentially missing signs of (partial) flap loss. iPPG-derived perfusion maps provide easy and complete visual representation of perfusion in the flap, potentially allowing for the identification of "cold zones" and potentially aiding in discarding inadequately perfused parts to avoid dehiscence or flap failure.

Ease of postoperative monitoring highly depends on the accessibility of the flap location for acquisition and can bring extra challenges in assessing flap recovery. A limitation of the current setup and the main barrier to making this technique easy to use is that only flaps that are within the field of view of the camera, which are mainly located in the face or anterior oral cavity, can be visualized. As a result, flaps located in the oropharynx are mostly inaccessible and subsequent postoperative monitoring is extremely difficult. This challenge will be addressed by introducing iPPG in smaller devices, such as flexible endoscopes to reach difficult accessible and remote areas within the oral cavity and oropharynx. This makes an easy and comfortable assessment of flap perfusion recovery in postoperative settings possible, without causing discomfort for the patient. Unfortunately, buried flaps, such as frequently occurring with muscle-only flaps, can only be assessed using this technique during the intraoperative phase and not during the postoperative monitoring phase. To further improve the usability of iPPG in clinical settings, feedback about perfusion should be displayed in real-time. Currently, image processing is performed offline after acquisitions. In addition, real-time feedback will also allow for continuous flap monitoring, supporting immediate intervention when indicated. Moreover, using iPPG to continuously monitor flap compromise might also be particularly useful for detecting subtle changes such as early venous congestion, as iPPG will be able to detect blood stasis by analysis of the delay time from the perfusion maps. In addition to iPPG, tissue oximetry devices, such as T-stat, are already in use for clinical care and display the clinical value of such devices. While out of the scope of this study to compare IPPG with other readily available techniques, it is imperative to do so in future work as it will provide crucial information on the needs for development and role of iPPG in clinical care.

iPPG brings several advantages in assessing perfusion in free flaps. iPPG is a software-based technique, providing the advantage that off-the-shelf cameras can be used for acquisition, and removing the need for expensive hardware upgrades. As such, iPPG is a low-cost and easily accessible for medical centers. iPPG is highly accurate in detecting microvasculature perfusion in the skin and has proven to detect even small perturbations in perfusion levels [11]. iPPG is a noninvasive technique with an easy-to-use user-interface for people without a technical background, removing the necessity of a technical assistant in the operating theaters or the postoperative setting. As such, residents and nurses will be able to perform iPPG acquisitions independently, and assess them on the spot. During acquisitions, visualization of the complete flap is possible,

and smaller ROIs can be selected for more detailed information from a single video. Acquisitions are fast (< 30 s) and provide almost immediate (< 1 min) feedback about the perfusion status to the clinician, supporting clinical decision making when immediate intervention is indicated.

iPPG offers significant advantages over traditional pin prick methods by providing noninvasive, continuous monitoring of tissue perfusion, reducing patient discomfort and infection risks. Its ability to assess blood flow across larger areas makes it particularly valuable for detecting perfusion issues in complex flap types, potentially preventing complications like ischemia. Although not extensively studied yet, iPPG shows promise in improving patient outcomes through early detection of microcirculation problems.

4 | Conclusion

iPPG is a simple and low-cost technique able to accurately detect microvascular perfusion in FFR surgeries. Together with the fact that large amounts of information is acquired from one single acquisition, iPPG is a promising new, noninvasive imaging technique in FFR surgeries, providing valuable intra-operative information about flap perfusion after revascularization. Although further research is needed, iPPG may have an additional benefit for flap monitoring in the postoperative period, providing easy-to-interpret perfusion maps of the flap, thereby potentially identifying vascular compromised flaps in an early stage and allowing timely intervention.

Acknowledgments

We wish to express our appreciation to Willem Verkruijsse, Principal Scientist at the department of Patient Care & Monitoring at Philips Research, who contributed to the development of the iPPG setup for the data acquisition, as well as proposed solutions for both motion compensation, data processing, and data interpretation. Additionally, we would like to thank the statisticians in the AVL-NKI for aiding in selecting the statistical analysis in this study. Marco Lai received funding from the European Union's Horizon 2020 Research and Innovation Program under Marie Skłodowska-Curie (Grant 721766) (FBI). website: https://ec.europa.eu/programmes/horizon2020/en. The funders had no role in the study design, data collection and analysis, decision to publish, or manuscript preparation.

Ethics Statement

The study was approved by the hospital's institutional review board.

Consent

Written informed consent was provided by each patient included in this study.

Conflicts of Interest

None of the authors who are affiliated with clinical institutions or universities (S.D.v.d.S., H.C.G., R.D., P.J.F.M.L., M.B.K., L.H.E.K., T.J.M.R., and W.H.S.) have financial interests in the subject matter, materials, or equipment or with any competing materials. The authors affiliated with Philips Research (M.L., M.v.G., and B.H.) have financial interests in the subject matter, materials, and equipment, in the sense that they are employees of Philips. Authors without conflicts of interest had full control of all data labeling, data analysis and information submitted for publication and over all conclusions drawn in the manuscript.

Data Availability Statement

The data sets generated during and/or analyzed during the current study are not publicly available.

References

1. U. A. Patel, D. Hernandez, Y. Shnayder, et al., "Free Flap Reconstruction Monitoring Techniques and Frequency in the Era of Restricted Resident Work Hours," *JAMA Otolaryngology–Head & Neck Surgery* 143, no. 8 (2017): 803–809, https://doi.org/10.1001/jamaoto.2017.0304.

2. K. T. Chen, S. Mardini, D. C. C. Chuang, et al., "Timing of Presentation of the First Signs of Vascular Compromise Dictates the Salvage Outcome of Free Flap Transfers," *Plastic and Reconstructive Surgery* 120, no. 1 (2007): 187–195, https://doi.org/10.1097/01.prs.0000264077.07779.50.

3. L. Vieira, D. Isacson, E. O. F. Dimovska, and A. Rodriguez-Lorenzo, "Four Lessons Learned From Complications in Head and Neck Microvascular Reconstructions and Prevention Strategies," *Plastic and Reconstructive Surgery—Global Open* 9, no. 1 (2021): e3329, https://doi.org/10.1097/gox.0000000000003329.

4. J. M. Smit, C. J. Zeebregts, R. Acosta, and P. M. N. Werker, "Advancements in Free Flap Monitoring in the Last Decade: A Critical Review," *Plastic and Reconstructive Surgery* 125, no. 1 (2010): 177–185, https://doi.org/10.1097/PRS.0b013e3181c49580.

5. C. Salgado, H. Chim, S. Schoenoff, and S. Mardini, "Postoperative Care and Monitoring of the Reconstructed Head and Neck Patient," *Seminars in Plastic Surgery* 24, no. 3 (2010): 281–287, https://doi.org/10.1055/s-0030-1263069.

6. A. Kapoor, M. Karmakar, C. Roy, and K. P. Anand, "Assessment of Perfusion of Free Flaps Used in Head and Neck Reconstruction Using Pulsatility Index," *Indian Journal of Plastic Surgery* 50, no. 2 (2017): 173–179, https://doi.org/10.4103/ijps.IJPS_23_17.

7. M. P. Chae, W. M. Rozen, I. S. Whitaker, et al., "Current Evidence for Postoperative Monitoring of Microvascular Free Flaps: A Systematic Review," *Annals of Plastic Surgery* 74, no. 5 (2015): 621–632, https://doi.org/10.1097/SAP.0b013e3181f8cb32.

8. A. Cornejo, T. Rodriguez, M. Steigelman, et al., "The Use of Visible Light Spectroscopy to Measure Tissue Oxygenation in Free Flap Reconstruction," *Journal of Reconstructive Microsurgery* 27, no. 7 (2011): 397–402, https://doi.org/10.1055/s-0031-1281521.

9. L. H. Kohler, H. Köhler, S. Kohler, et al., "Hyperspectral Imaging (HSI) as a New Diagnostic Tool in Free Flap Monitoring for Soft Tissue Reconstruction: A Proof of Concept Study," *BMC Surgery* 21, no. 1 (2021): 222, https://doi.org/10.1186/s12893-021-01232-0.

10. A. A. M. A. Lindelauf, A. G. Saelmans, S. M. J. van Kuijk, R. R. W. J. van der Hulst, and R. M. Schols, "Near-Infrared Spectroscopy (NIRS) Versus Hyperspectral Imaging (HSI) to Detect Flap Failure in Reconstructive Surgery: A Systematic Review," *Life* 12, no. 1 (2022): 65, https://doi.org/10.3390/life12010065.

11. M. Lai, C. D. Spiridione, M. de Wild, et al., "Evaluation of a Non-Contact Photo-Plethysmographic Imaging (iPPG) System for Peripheral Arterial Disease Assessment," in *Proceedings of the SPIE 11600, Medical Imaging 2021: Biomedical Applications in Molecular, Structural, and Functional Imaging* (SPIE, 2021), 116000F, https://doi.org/10.1117/12.2580640.

12. M. Lai, C. Shan, C. Ciuhu-Pijlman, and M. Izamis, "Perfusion Monitoring by Contactless Photoplethy Smography Imaging," in *2019*

IEEE 16th International Symposium on Biomedical Imaging (ISBI 2019) (Venice, Italy, 2019), 1778–1782, https://doi.org/10.1109/ISBI.2019.8759547.

13. D. Chubb, W. M. Rozen, and M. W. Ashton, "Early Survival of a Compromised Fasciocutaneous Flap Without Pedicle Revision: Monitoring With Photoplethysmography," *Microsurgery* 30 (2010): 462–465, https://doi.org/10.1002/micr.

14. T. Zaman, P. A. Kyriacou, and S. K. Pal, "Free Flap Pulse Oximetry Utilizing Reflectance Photoplethysmography," *Annual International Conference of the IEEE Engineering in Medicine and Biology Society* 2013 (2013): 4046–4049, https://doi.org/10.1109/EMBC.2013.6610433.

15. M. Lai, S. D. van der Stel, H. C. Groen, et al., "Imaging PPG for in Vivo Human Tissue Perfusion Assessment During Surgery," *Journal of Imaging* 8, no. 4 (2022): 94.

16. D. Dindo, N. Demartines, and P. A. Clavien, "Classification of Surgical Complications: A New Proposal With Evaluation in a Cohort of 6336 Patients and Results of a Survey," *Annals of Surgery* 240, no. 2 (2004): 205–213, https://doi.org/10.1097/01.sla.0000133083.54934.ae.

17. T. Xiao, Z. Yan, S. Xiao, and Y. Xia, "Proinflammatory Cytokines Regulate Epidermal Stem Cells in Wound Epithelialization," *Stem Cell Research & Therapy* 11, no. 1 (2020): 232, https://doi.org/10.1186/s13287-020-01755-y.

18. W. Z. Wang, "Investigation of Reperfusion Injury and Ischemic Preconditioning in Microsurgery," *Microsurgery* 29 (2009): 72–79, https://doi.org/10.1002/micr.20587.

19. K. D. Wolff, "New Aspects in Free Flap Surgery: Mini-Perforator Flaps and Extracorporeal Flap Perfusion," *Journal of Stomatology, Oral and Maxillofacial Surgery* 118, no. 4 (2017): 238–241, https://doi.org/10.1016/j.jormas.2017.06.004.

20. K. D. Wolff, L. M. Ritschl, A. von Bomhard, C. Braun, C. Wolff, and A. M. Fichter, "In Vivo Perfusion of Free Skin Flaps Using Extracorporeal Membrane Oxygenation," *Journal of Cranio-Maxillofacial Surgery* 48, no. 1 (2020): 90–97, https://doi.org/10.1016/j.jcms.2019.12.005.

21. W. Wang, A. Ong, A. G. Vincent, T. Shokri, B. Scott, and Y. Ducic, "Flap Failure and Salvage in Head and Neck Reconstruction," *Seminars in Plastic Surgery* 34, no. 4 (2020): 314–320, https://doi.org/10.1055/s-0040-1721766.

22. Y. Foerster, L. Baumann, I. Kafantari, et al., "Recipient Bed Perfusion as a Predictor for Postoperative Complications in Irradiated Patients With Microvascular Free Tissue Transfer of the Head and Neck Area: A Clinical Analysis of 191 Microvascular Free Flaps," *Oral and Maxillofacial Surgery* 27 (2022): 313–323, https://doi.org/10.1007/s10006-022-01070-1.

23. K. H. Chen, S. C. H. Kuo, P. C. Chien, H. Y. Hsieh, and C. H. Hsieh, "Comparison of the Surgical Outcomes of Free Flap Reconstruction for Primary and Recurrent Head and Neck Cancers: A Case-Controlled Propensity Score-Matched Study of 1,791 Free Flap Reconstructions," *Scientific Reports* 11, no. 1 (2021): 2350, https://doi.org/10.1038/s41598-021-82034-5.

24. R. M. Kwasnicki, A. J. Noakes, N. Banhidy, and S. Hettiaratchy, "Quantifying the Limitations of Clinical and Technology-Based Flap Monitoring Strategies Using a Systematic Thematic Analysis," *Plastic and Reconstructive Surgery—Global Open* 9, no. 7 (2021): 1–8, https://doi.org/10.1097/GOX.0000000000003663.